ELSEVIER

Journal of Petroleum Science and Engineering 35 (2002) 151–166

JOURNAL OF PETROLEUM SCIENCE & ENGINEERING

www.elsevier.com/locate/jpetscieng

Efficient global optimization for hydraulic fracturing treatment design

Néstor V. Queipo [a,*], Alexander J. Verde [a], José Canelón [b], Salvador Pintos [a]

[a] *Applied Computing Institute, Faculty of Engineering, University of Zulia, Venezuela*
[b] *Electrical Engineering School, Faculty of Engineering, University of Zulia, Venezuela*

Received 12 March 2001; accepted 15 March 2002

Abstract

This paper presents a methodology for the optimal hydraulic fracture treatment design. The methodology includes the construction of a "fast surrogate" of an objective function whose evaluation involves the execution of a time-consuming computational model, based on neural networks, DACE modeling, and adaptive sampling. Using adaptive sampling, promising areas are searched considering the information provided by the surrogate model and the expected value of the errors. The proposed methodology provides a global optimization method, hence avoiding the potential problem of convergence to a local minimum in the objective function exhibited by the commonly Gauss–Newton methods. Furthermore, it exhibits an affordable computational cost, is amenable to parallel processing, and is expected to outperform other general purpose global optimization methods such as simulated annealing and genetic algorithms. The methodology is evaluated using two case studies corresponding to formations differing in rock and fluid properties, and geometry parameters. From the results, it is concluded that the methodology can be used effectively and efficiently for the optimal design of hydraulic fracture treatments.

Keywords: Bayesian global optimization; Hydraulic fracture design; Surrogate modeling-based optimization

1. Introduction

Hydraulic fracturing is one of the most common stimulation strategies used to enhance the production from oil and gas wells. During a hydraulic fracturing treatment, fluids are injected to the formation at a pressure high enough to cause tensile failure of the rock and propagate the fracture. As a result of a successful treatment, a path with much higher permeability than the surrounding formation is created from the well. Each of the fluids injected during the treatment execution performs a significant and specific task. The initial fluid, known as pad, initiates and propagates the fracture. The following stages of the treatment involve the injection of a fracturing fluid with varying concentrations of proppant. The fluid is intended to continue the fracture propagation and the proppant will keep the fracture open, even though the formation stresses will try to close the fracture after the fluid injection ceases.

For a given formation, the design of a hydraulic fracture treatment involves the selection of appropriate fracturing fluids and proppants, the number of

* Corresponding author. MCO: 459, 4440 N.W., 73 Av., 33166 Miami, FL, USA. Tel.: +58-61-598630; fax: +58-61-934080.
E-mail address: nqueipo@luz.ve (N.V. Queipo).

0920-4105/02/$ - see front matter
PII: S0920-4105(02)00237-1

treatment stages, the concentrations and the rates and pressures of injection of each stage. Each design will result in a specific fracture geometry and conductivity, which is related to the production increase obtained from the fractured well. This means that, due to the several possible combinations of the parameters involved and their nonlinear interactions, there are a significant number of possible fracture geometries, each of which will result in a different post-fracture well production performance.

Ralph and Veatch (1986) present the general concepts of hydraulic fracture treatments economics and introduce the net present value as a valuable tool for the optimal design of hydraulic fracture treatment. An optimal hydraulic fracture treatment design maximizes the net present value of the revenue after the treatment, considering the post-fracture production performance and the treatment costs.

Table 1 presents a summary of previous work in the area of hydraulic fracture optimization. Poulsen and Soliman (1986) used fluid volume and proppant concentration as treatment design variables, with a two-dimensional fracture propagation model, accounting for proppant transport and sedimentation. No formal optimization procedure was used (trial and error), minimizing the difference between calculated and desired fracture length and conductivity. Balen et al. (1988) used as design variables the fracturing fluid, injected fluid volume and proppant concentration, pumping rate, and proppant types. Their work used a two-dimensional fracture propagation model for predicting fracture geometry and an economic model. The optimization procedure was based on a sensitivity analysis of the design variables with respect to net present value. Hareland et al. (1993) used fluid injection rate and fracturing fluid as design variables and a pseudo three-dimensional fracture propagation model coupled with a post-fracture production and economic models. The optimization procedure was similar to that used by Balen et al. (1988). Rueda et al. (1994) considered as treatment design variables the injected fluid volume, fracturing fluid type, proppant type, and pumping rate. Their work used a two-dimensional fracture propagation model, accounting for fracture closure behavior, and a post-fracture production model coupled with an economic model. The optimization was posed as a mixed integer linear programming (MILP) problem and solved accordingly. Mohaghegh et al. (1999) used as design variables the fluid volume injected, proppant concentration, and fluid injection rate. Their work used a surrogate model of a three-dimensional fracturing simulator accounting for fracture propagation and closure behavior, and proppant transport and sedimentation. The optimization procedure was a Genetic Algorithm.

The analysis of previous work shows limitations such as the absence of a global optimization procedure (Poulsen and Soliman, 1986; Balen et al., 1988; Hareland et al., 1993; Rueda et al., 1994), direct coupling of the hydraulic fracture models and optimization procedure (Poulsen and Soliman, 1986; Balen et al., 1988; Hareland et al., 1993), no error estimation (all the previous work), limited number of design variables (Poulsen and Soliman, 1986; Hareland et al., 1993), not account for fracture closure and proppant transport and sedimentation (Poulsen and Soliman, 1986; Balen et al., 1988; Hareland et al., 1993), and not include an economic model (Poulsen and Soliman, 1986; Mohaghegh et al., 1999).

This paper presents a methodology called neural network-based efficient global optimization (NEGO) developed by Queipo et al. (2000), for the optimal design of hydraulic fracture stimulation treatments. This methodology includes the construction of a "fast surrogate" of an objective function, whose evaluation involves the execution of a time-consuming computational model (hydraulic fracture simulator), based on neural networks, DACE (Sacks et al., 1989), modeling, and adaptive sampling. Using adaptive sampling, promising areas are searched considering the information provided by the surrogate model and the expected value of the errors.

The DACE surrogate model is initially constructed using sample data generated from the execution of the computational model with parameters given by a Latin hypercube experimental design and a neural network, and provides error estimates at any point. Additional points are obtained balancing the exploitation of the information provided by the surrogate model (where the surface is minimized) with the need to improve the surface (where error estimates are high). The proposed methodology provides a global optimization method, hence avoiding the potential problem of convergence to a local minimum in the objective function exhibited by the commonly used Gauss–Newton methods, and the computational cost

Table 1
Summary of previous work in the area of hydraulic fracture optimization

Authors	Design variables	Objective function	Models	Optimization procedure	Surrogate models	Error estimation
Poulsen and Soliman (1986)	• Injected fluid volume • Proppant concentration	Minimization of the difference between desired and calculated fracture length and conductivity	• Two-dimensional fracture propagation • Proppant transport and sedimentation	Heuristic	No	No
Balen et al. (1988)	• Injected fluid volume • Proppant concentration • Fluid injection rate • Proppant types • Fracturing fluid	Maximization of the net present value	• Two-dimensional fracture propagation • Economic model	Search assisted using sensitivity analysis	No	No
Hareland et al. (1993)	• Fluid injection rate • Fracturing fluid	Maximization of the net present value	• Pseudo three dimensional fracture propagation • Post-fracture production • Economic model	Search assisted using sensitivity analysis	No	No
Rueda et al. (1994)	• Injected fluid volume • Fracturing fluid • Proppant types • Fluid injection rate	First case: Maximization of the net present value Second case: Minimization the fracture treatment costs	• Two-dimensional fracture propagation • Fracture closure • Post-fracture production • Economic model	Mixed Integer Linear programming Technique (MILP)	No	No
Mohaghegh et al. (1999)	• Injected fluid volume • Proppant concentration • Fluid injection rate	Minimization of the difference between desired and calculated fracture length and conductivity	• Surrogate model of a three-dimensional fracturing simulator taking account: • Fracture propagation • Fracture closure • Proppant transport and sedimentation	Genetic algorithms	Yes	No
Queipo et al. (2000) (present work)	• Injected fluid volume • Proppant concentration • Fluid injection rate • Fracturing fluid	Maximization of the net present value	• Two-dimensional fracture propagation • Fracture closure • Proppant transport and sedimentation • Post-fracture production • Economic model	Neural Network based Efficient Global Optimization (NEGO)	Yes	Yes

involved in numerically estimating derivatives and in the step-by-step movement along given trajectories. Furthermore, it exhibits an affordable computational cost, is amenable to parallel processing, and is expected to outperform other general purpose global optimization methods such as simulated annealing and genetic algorithms.

2. Problem definition

The problem of interest is an optimization problem with a typically high number of design parameters and computationally expensive objective function evaluations. Formally, it can be stated as:

find $x \in X \subseteq \mathbf{R}^p$

such that

$f(x)$ is minimized

where f is an objective function of x, the design variables of a fracture treatment, and X is a set of constraints. The design vector $\boldsymbol{x}$, is given by:

- Volume of the stages (V_1, V_2,. . ., V_n)
- Proppant concentration increment for the last n stages (ΔCp_{21}, ΔCp_{32},. . .,ΔCp_{jh} where $j=2,\ldots, n$; $h=1,\ldots, n-1$)
- Fracturing fluid injection rate (Q_i)
- Fluid performance index (n_p)
- Consistency index K_f

and the set of constraints is:

$$x_{i\,\min} \leq x_i \leq x_{i\,\max} \qquad \text{from } i = 1,2\ldots m$$

where: $x_{i\,\max}$: upper bound; $x_{i\,\min}$: lower bound.

Hence, the problem is to find, for a given formation, the fracture treatment design that will maximize the net present value of the post-fracture revenue, considering the well post fracture production performance and the treatment costs. The formation is characterized by the following parameters:

- Poisson ratio (υ)
- Young's modulus (E)
- Stress in the pay-zone (σ_p)
- Pay-zone height (H_p)
- Reservoir permeability (k_r)
- Reservoir outer boundary radius (r_e)
- Wellbore radius (r_w)
- Spurt-loss coefficient (S_p)
- Leak-off coefficient (C).
- Oil volumetric factor (B_o).
- Flowing bottomhole pressure (P_{wf})
- Reservoir initial pressure (P_i)
- Oil viscosity (μ_o)

The objective function is given by:

$$f(x) = -\mathrm{NPV}(x) \tag{1}$$

where, NPV is the net present value of the post-fracture revenue.

To calculate the NPV associated with a specific fracture treatment, it is typically necessary to execute a time consuming computational model that includes a hydraulic fracture simulator, a post fracturing production model, and an economical model. This issue places restrictions on the solution approach, given that the number of objective function evaluations is limited to a relatively low value considering the time restrictions typically present in the oil industry.

3. Solution methodology

The optimization strategy includes the construction of a "fast surrogate" of an objective function, whose evaluation involves the execution of a computational model, which estimates the net present value of the revenue for a specific fracture treatment. The computational model integrates a hydraulic fracture simulator, a production model, and an economic model.

The hydraulic fracture simulator computes, for a given formation, the fracture geometry and conductivity resulting from a specific treatment. In this study, the simulator is based on the GDK (Geertsma and de Klerk, 1969) 2D fracture propagation model, and includes models for proppant transport and sedimentation (Domselaar and Visser, 1974; Daneshy, 1978), and for the closure behavior of the fracture (Nolte, 1979; Novotny, 1977). The production model (Raymond and Binder, 1967) estimates the post-treatment well production according to the increment of the productivity index. The economic model (Ralph and

Veatch, 1986) calculates the net present value of the revenue, considering a production time horizon and treatment costs.

3.1. Hydraulic fracture simulator

The inputs to the simulator are the formation parameters and the treatment design variables. The simulator computes the fracture geometry and the proppant transport and sedimentation, during propagation and closure of the fracture. This information is used to calculate the ratio of post-fracture and pre-fracture productivity indexes. For a successful treatment this ratio is greater than 1.

This work uses the GDK 2D propagation model (Geertsma and de Klerk, 1969), which assumes constant fracture height during propagation. The simulator solves a coupled system of partial differential equations, which model the different physical phenomena involved in the hydraulic fracturing process.

3.1.1. Model equations

3.1.1.1. Fracture geometry. Geertsma and de Klerk (1969) present the equations that model the fracture geometry. According to the mass conservation principle, the mass injected to the fracture must equal the sum of the mass accumulated in it and the mass that is lost due to formation porosity, known as leak-off. Considering as incompressible the fracturing fluid and the leak-off and spurt loses, the relationship between the fluid flow Q and the cross section A of the fracture is expressed by:

$$-\frac{\partial Q(x,t)}{\partial x} = Q_L(x,t) + \frac{\partial A(x,t)}{\partial t} \tag{2}$$

where the loses Q_L are given by:

$$Q_L(x,t) = \frac{2CH_p}{\sqrt{t-\tau(x)}} + 2S_pH_p\frac{\partial}{\partial x}\left(\frac{\partial L}{\partial t}\right) \tag{3}$$

Assuming a linear propagation of the fracture, the width W of the fracture is given by:

$$W(x,t) = \frac{4(1-\upsilon^2)P(x,t)L}{E} \tag{4}$$

This means that at any time, the width is constant in a vertical section of the fracture.

If one-dimensional and stable flow is assumed, the relationship between the flow rate through a vertical section and the pressure gradient along the fracture propagation direction is specified as:

$$\frac{\partial P(x,t)}{\partial x} = \frac{\eta Q(x,t)^{n_p}}{W(x,t)^{2n_p+1}H^{n_p}} \tag{5}$$

where η is given by

$$\eta = 2^{(n_p+1)}K_f\left(2+\frac{1}{n_p}\right)^{n_p} \tag{6}$$

The fracture geometry during propagation is obtained by solving Eqs. (2), (4) and (5) subject to the following:

$$\begin{aligned} &\text{Initial condition :} && W(x,0) = 0 \\ &\text{Boundary conditions :} && Q(0,t) = Q_i/2 \\ & && W(L,t) = 0 \end{aligned} \tag{7}$$

3.1.1.2. Proppant transport and sedimentation. The proppant are spherical solid particles that prevent the fracture closure after the injection ceases. Without a loss of generality, it will be considered treatments of one stage of pad injection and a maximum of four stages of mixed fluid and proppant injection. The proppant concentration of the injection fluid at each stage, denoted by Cp_i $i=1,\ldots,5$ is constant, with $Cp_1=0$ (fluid without proppant) and $Cp_2 \le Cp_3 \le Cp_4 \le Cp_5$. However, the proppant concentration along the fracture increases because of leak-off and fracture volume reduction. It is necessary to calculate the proppant concentration along the fracture at any time.

Domselaar and Visser (1974) suggest the following equation,

$$Q(x,t)\frac{\partial \overline{C}p(x,t)}{\partial x} + A(x,t)\frac{\partial \overline{C}p(x,t)}{\partial t} - \overline{C}p(x,t)Q_L(x,t) = 0 \tag{8}$$

which can be solved numerically to obtain the normalized proppant concentration $\overline{C}p$ profile along the fracture at any time. Suppose that at time t, the pad stage and two stages of proppant mixtures have been injected into the fracture. It is assumed that different

stages do not mix. This situation is illustrated in Fig. 1, in which each number identifies one injection stage. The normalized proppant concentration at time t of any point x in a proppant mixture injection stage, denoted by $\overline{C}\,p(x,t)$, is defined as the ratio of the concentration $Cp(x,t)$ at that point, to the concentration at with the stage was injected. For point x_1 in Fig. 1:

$$\overline{C}p(x_1,t) = \frac{Cp(x_1,t)}{Cp_2}. \tag{9}$$

A mass balance is used to locate the contact between two consecutive stages, known as proppant fronts. The proppant concentration $Cp(x,t)$, computed with the normalized proppant concentration $\overline{C}\,p(x,t)$ and the proppant front locations, are used to calculate the descend velocity of the proppant particles suspended in the fluid, according to Eq. (10):

$$V_s(x,t) = \frac{(2n_p+1)d}{108n_p}\left[\frac{(\rho_p-\rho_f)}{72\mu_a}\right]^{\frac{1}{n_p}}\frac{(1-Cp(x,t))^2}{10^{1.82(1-Cp(x,t))}} \tag{10}$$

where μ_a, known as apparent fluid viscosity, is given by,

$$\mu_a = K_f\left(\frac{2n_p+1}{3n_p}\right)^{n_p}. \tag{11}$$

Some of the descending proppant particles will group on the bottom of the fracture, forming what is known as proppant bed, and some will become trapped between the fracture lateral walls after closure. Smaller closure times and/or lower descend velocities increase the number of particles trapped by the fracture walls, which is a desirable feature because the resulting fractured producing zone will be greater. Daneshy (1978) developed a numerical solution procedure to calculate the volume of the proppant bed and the volume of suspended proppant, from the descend velocity of proppant particles. These results and the fracture closure time were used in this work to determine the volume of proppant trapped between fracture walls.

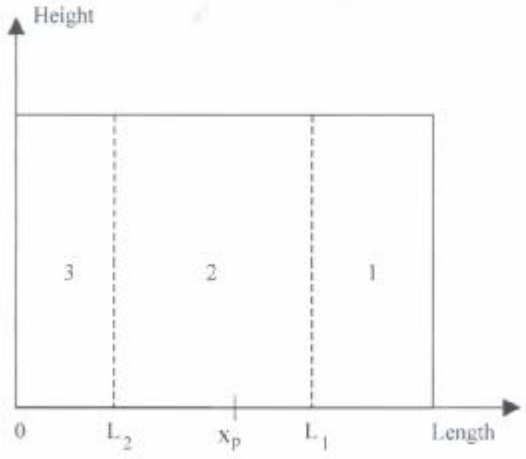

Fig. 1. Illustration for proppant concentration calculation.

3.2. Post-fracture production model

This model calculates the productivity index ratio and cumulative oil production.

3.2.1. Productivity indexes ratio calculation

The post-fracture productivity index depends on the geometry after the fracture has closed. This geometry is obtained by solving Eq. (1) during closure time, with $Q(x,t)=0$ and assuming that the fracture width and height decrease at the same rate. The cross section of the fracture at any x has a rectangular shape.

The post-fracture and pre-fracture productivity indexes ratio is calculated by applying the equation developed by Raymond and Binder (1967), to the propped fracture divided in N intervals of the same length along its propagation direction:

$$\frac{J}{J_o} = \frac{\ln\left(\frac{r_e}{r_w}\right)}{\left\{\sum_{i=1}^{N}\ln\left[\frac{\pi L(i)+W_{eff}(i)\left(\frac{H_{eff}(i)K_p(i)}{H_f K_f}\right)}{\pi L(i-1)+W_{eff}(i-1)\left(\frac{H_{eff}(i-1)K_p(i-1)}{H_f K_f}\right)}\right]\right\}+\ln\left(\frac{r_e}{r_w}\right)} \tag{12}$$

where $L(i)$, $W_{eff}(i)$, $H_{eff}(i)$ and $K_p(i)$ are the length, width, height, and proppant permeability evaluated in the ith element.

3.2.2. Cumulative oil production calculation

The production rate just before the treatment is calculated using Darcy's Law for semi-stable flow:

$$Q_o = \frac{2\pi K_r H_p(\overline{P}-P_{wf})}{B_o\mu_o \mathrm{Ln}\left(0.472\frac{r_e}{r_w}\right)} \tag{13}$$

The initial production rate after the fracture treatment, denoted by Q_{of}, is given by

$$Q_{of} = Q_o J / J_o \tag{14}$$

To estimate the post-treatment production rate performance, it is assumed a hyperbolic decline curve:

$$Q(t) = Q_{of}(1 + m a_i t)^{-1/m} \tag{15}$$

where a_i is the initial declination rate and m is a constant such that $0 < m < 1$.

Defining t_{of} as the initial after the treatment and a time horizon of T years, the cumulative oil production in BBL during that time horizon, denoted by COP, is given by

$$\mathrm{COP} = \int_{t_{of}}^{t_{of}+T} Q(t)\mathrm{d}t = \int_{t_{of}}^{t_{of}+T} \times Q_{of}(1 + m a_i t)^{-1/m}\mathrm{d}t. \tag{16}$$

3.3. Economic model

The net present value of the revenue ($\mathrm{NPV_{rev}}$) produced by the fracture treatment is calculated, which is given by:

$$\mathrm{NPV_{rev}} = \mathrm{NPV_{inc}} - \mathrm{NPV_{cost}} \tag{17}$$

where $\mathrm{NPV_{inc}}$ is the net present value of the income, considering the cumulative oil production and the oil barrel price, and $\mathrm{NPV_{cost}}$ is the net present value of the total costs, which include treatment costs, operational costs, and production duties.

3.4. Optimization strategy

The proposed solution approach called NEGO, neural-network based efficient global optimization, is an improved version of the EGO algorithm (Matlab, Ver. 5.3) for the optimization of computationally expensive black-box functions.

The proposed solution methodology involves the following five steps:

(1) Constructing a sample of the parameter space using the Latin hypercube method. The Latin hypercube sampling procedure has been shown to be very effective for selecting input variables for the analysis of the output of a computer code (Queipo et al., 2000).

(2) Conducting computer model executions using the sample from the previous step and recording the objective function values.

(3) Constructing a parsimonious neural network using the data from the previous step. The purpose of this neural network is to capture the general trends observed in the data; no rigorous performance criteria is placed on the neural network. The input variables of the neural network are the fracture treatment design parameters and the output variable is the corresponding objective function value.

(4) Constructing a DACE model for the residuals, that is, the difference between the observed objective function values, and the neural network responses using the sample data. These models provide not only estimates of the residuals values but also of the respective errors. The surrogate model for the evaluation of the objective function is the sum of the neural network and DACE models. Details of this step will be given later in this section.

(5) Additional points are obtained balancing the exploitation of the information provided by the surrogate model (where the surface is minimized) with the need to improve the surface (where error estimates are high), until stopping criteria have been met. This balance is achieved by sampling where a figure of merit is maximized. Details of the figure of merit will be given later in this section.

3.4.1. DACE models

These models owe their name, design, and analysis of computer experiments to the title of an article that popularized the approach (Sacks et al., 1989). These models suggest to estimate deterministic functions as shown in Eq. (18):

$$y(x_j) = \mu + \varepsilon(x_j) \tag{18}$$

where, y is the function to be modeled, μ is the mean of the population, and ε is the error with zero expected value, and with a correlation structure given by:

$$\mathrm{cov}(\varepsilon(x_i),\varepsilon(x_j)) = \sigma^2 \exp\left(-\sum_{h=1}^{p} \theta_h (x_i^h - x_j^h)^2\right) \tag{19}$$

where, p is the dimension of vector x, σ identifies the standard deviation of the population, and, θ_h is a

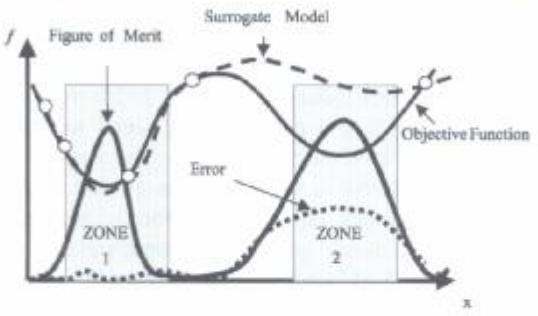

Fig. 2. Illustration of the purpose of the figure of merit.

correlation parameter, which is a measure of the degree of correlation among the data along the h direction.

Specifically, given a set of n input/output pairs (x, f), the parameters, μ, σ, and θ are estimated such that the likelihood function is maximized (Sacks et al., 1989). Having estimated these values, the function estimate for new points is given by

$$\bar{y}(x) = \bar{\mu} + \boldsymbol{r}^t\, \mathbf{R}^{-1}(y - L\bar{\mu}) \tag{20}$$

where, the line above the letters denote *estimates*, $\boldsymbol{r}^t$ identifies the correlation vector between the new point and the points used to construct the model, $\mathbf{R}$ is the correlation matrix among the $\boldsymbol{n}$ sample points, and L denotes an n-vector of ones.

The mean square error of the estimate is given by:

$$s^2(x^*) = \sigma^2\left[1 - \boldsymbol{r}^t\, \mathbf{R}^{-1} r + \frac{(1 - L^t\, \mathbf{R}^{-1} r)}{L^t\, \mathbf{R}^{-1} L}\right] \tag{21}$$

The model is validated through a cross-validation procedure, which essentially makes sure that the estimates using all but the point being tested and the actual response values are within an specified number of standard deviations. That is, the matrix $\mathbf{R}$ used to compute the function and standard deviation estimates does not include the point being tested. The original EGO algorithm may not cross-validate properly if there are trends in the data, in contrast to NEGO which is expected to subtract any significant trends in the data. More precisely, the EGO algorithm expects the data to be trendless and the correlation structure of the errors to be only a function of the distance vector between points. When there are trends in the data (as is frequently the case), this assumption fails, and the model will not validate. The NEGO algorithm subtracts possible trends in the data using a neural network model.

The benefits of modeling deterministic functions using this probabilistic approach are: (i) represents a best linear unbiased estimator, (ii) interpolates the data, and (iii) provides error estimates.

3.4.2. Figure of merit

The figure of merit (more precisely a function of merit) reflects a balance of the influence of low function values and uncertainty. Specifically, the figure of merit (Jones et al., 1998) used in this work is given by:

$$\mathrm{fom}(x) = (f_{\min} - \hat{f})\Phi\left(\frac{f_{\min} - \hat{f}}{s}\right) + s\phi\left(\frac{f_{\min} - \hat{f}}{s}\right) \tag{22}$$

where Φ and ϕ are the cumulative and density normal distribution functions, respectively; $f_{\min}$ and $\hat{f}$ are the minimum current and objective function estimate value, respectively. Eq. (22) establishes the desired balance of sampling where the response surface (the predictor) is minimized (left term) and in zones where error estimates are high (right term). Note that the figure of merit makes reference to the objective

Table 2
Reservoir properties (Case Study 1)

Variable	Unit	Value
υ	(−)	0.3
E	(psi)	5.1^6
σ_p	(psi)	4000
H_p	(ft)	80
k_r	(md)	1
r_e	(ft)	2000
r_w	(in)	4
S_p	(gal/ft^2)	0.02
C	(ft/min)$^{1/2}$	0.00
B_w	(bbl/bb)	1.1
P_w	(psi)	800
P_i	(psi)	4000
μ_o	(cp)	2

Table 3
Reservoir properties (Case Study 2)

Variable	Unit	Value
v	(adim)	0.30
E	(psi)	5.10^5
σ_p	(psi)	6000
H_p	(ft)	120
k_r	(md)	0.1
r_e	(ft)	1500
r_w	(in)	4
S_p	(gal/ft^2)	0.04
C	(ft/min$^{1/2}$)	0.003
B_o	(bbl/Bbl)	1.2
P_{wf}	(psi)	1000
P_i	(psi)	6000
μ_o	(cp)	1

function, so it includes the sum of the output of both the neural network and the residual models.

Fig. 2 illustrates a possible figure of merit of one variable. There are two zones where it is desirable to add additional points: the zone (left) where the objective function is minimized and the zone (right) where there is a significant error in the prediction. Hence, the figure of merit for adding sample points should be high in either of these situations.

This surface response approach for global optimization is expected to outperform competing methods, in terms of necessary computationally expensive objective function evaluations, to meet a stopping criterion. It can identify promising areas without the need of moving step by step along a given trajectory. In addition, by providing estimates of the errors at unsampled points, it is possible to establish a reasonable stopping criterion. Furthermore, provides a fast surrogate model that could be used to visualize the relationship between the sought parameters and the objective function values and to identify the relative significance of each of the parameters.

3.4.3. Implementation

The following case studies were solved using an implementation of the NEGO algorithm in Matlab Ver. 5.3. The subproblems of finding near optimal values for maximizing likelihood and the figure of merit were solved using the DIRECT method (Jones et al., 1993). Note that the solution of these subproblems do not require additional computationally expensive objective function evaluations. The computer model was developed by the authors, also in Matlab Ver. 5.3.

4. Case studies

The proposed methodology was evaluated using two case studies, corresponding to formations differing in rock and fluid properties, and geometric parameters. The formation parameters for Case Studies 1 and 2 are shown in Tables 2 and 3, respectively. The fracture height for Case Study 1 (Case Study 2) was assumed to be 80 ft (180 ft) with a pay zone height of 80 ft (120 ft).

Table 4
Fracturing fluid density, and proppant types, diameters, densities and permeabilities (Case Study 1)

Fracturing fluid	
Density	1000 kg/m^3
Proppant for stages 2 and 3	
Type	20–40 Mesh Bauxite
Diameter	0.025 in.
Density	160 lb/ft^3
Permeability	450 d at 4000 psi
Proppant for stages 4 and 5	
Type	12–20 Mesh Bauxite
Diameter	0.055 in.
Density	160 lb/ft^3
Permeability	2200 d at 4000 psi

Table 5
Fracturing fluid density, and proppant types, diameters, densities and permeabilities (Case Study 2)

Fracturing fluid	
Density	1000 kg/m^3
Proppant for stages 2 and 3	
Type	20–40 Mesh Bauxite
Diameter	0.025 in.
Density	160 lb/ft^3
Permeability	400 d at 4000 psi
Proppant for stages 4 and 5	
Type	12–20 Mesh Bauxite
Diameter	0.055 in.
Density	160 lb/ft^3
Permeability	1400 d at 4000 psi

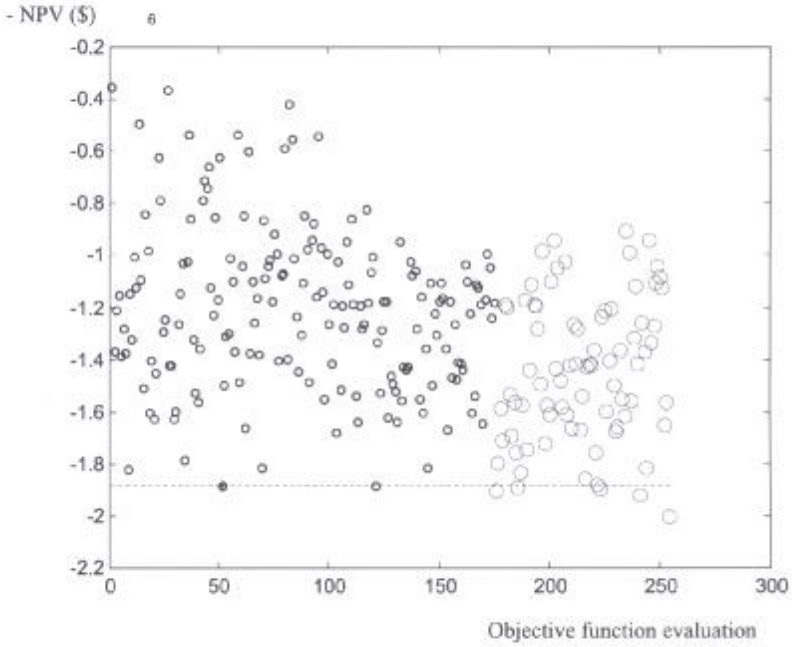

Fig. 3. Values of the objective function for Case Study 1.

As stated before, the problem is to find, for each formation, the fracture treatment design that will maximize the net present value of the post-fracture revenue. Specifically, the design vector, $\boldsymbol{x}$, is given by the fracture treatment parameters:

- Volume of the stages (V_1, V_2, V_3, V_4, V_5).
- Proppant concentration increment for the last four stages (ΔCp_{21}, ΔCp_{32}, ΔCp_{43}, ΔCp_{54}).
- Fracturing fluid injection rate (Q_i).
- Fluid performance index (n_p).
- Consistency index (K_f).

and the set of constraints is given by:

$$100 \text{ bbl} \le V_k \le 500 \text{ bbl} \quad k = 1, \ldots, 5$$
$$0 \text{ lbm/gal} \le \Delta Cp_{jh} \le 4 \text{ lbm/gal} \quad j = 2, \ldots, 5, \quad h = 1, \ldots, 4$$
$$10 \text{ bpm} \le Q_i \le 50 \text{ bpm}$$
$$0.3 \le n_p \le 1$$
$$0.0021 \text{ lbf s}^{n_p}/\text{ft}^2 \le K_f \le \text{lbf s}^{n_p}/\text{ft}^2$$

The following assumptions hold: (i) any fracture treatment is constituted by a first stage of pad injec-

Table 6
Best five values of the objective function found by the NEGO algorithm (Case Study 1)

#Iter	V_1 (bbl)	V_2 (bbl)	V_3 (bbl)	V_4 (bbl)	V_5 (bbl)	ΔCp_{21} (lbm/gal)	ΔCp_{32} (lbm/gal)	ΔCp_{43} (lbm/gal)	ΔCp_{54} (lbm/gal)	Q_i (bpm)	n_p (–)	K_f (lbf s^{n_p}/ft^2)	y × 10^6 ($)
1	433.33	166.66	300.00	433.33	433.33	2.00	2.00	2.00	2.00	43.33	0.650	0.0116	−1.903
11	433.33	166.66	300.00	166.66	433.33	2.00	2.00	2.00	2.00	43.33	0.650	0.0116	−1.887
48	433.33	300.00	166.66	433.33	433.33	2.00	2.00	2.00	2.00	43.33	0.650	0.0116	−1.896
66	433.33	166.66	166.66	433.33	300.00	2.00	2.00	2.00	2.00	43.33	0.650	0.0116	−1.911
79	433.33	300.00	300.00	433.33	300.00	3.33	2.00	3.33	2.00	43.33	0.650	0.0116	−2.000

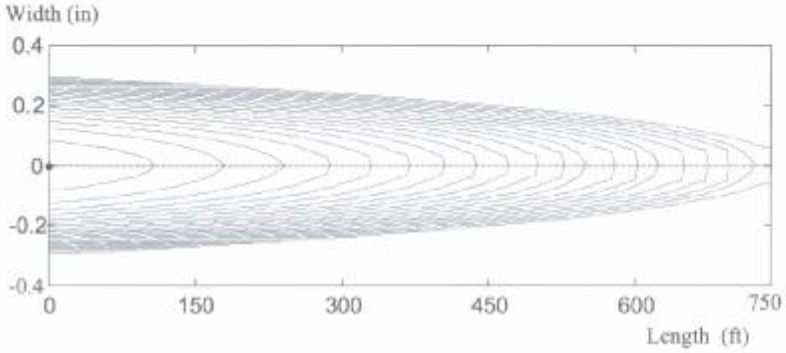

Fig. 4. Fracture width propagation during fluid injection for Case Study 1.

tion and a maximum of four stages of mixed fluid and proppant injection and (ii) fluid and proppant densities, and proppant types, diameters and permeabilities are known. Tables 4 and 5 show the corresponding values for Case Studies 1 and 2, respectively.

5. Results and discussion

5.1. Case Study 1

Using a Latin hypercube experimental design, an initial sample of 175 points in the 12-dimensional

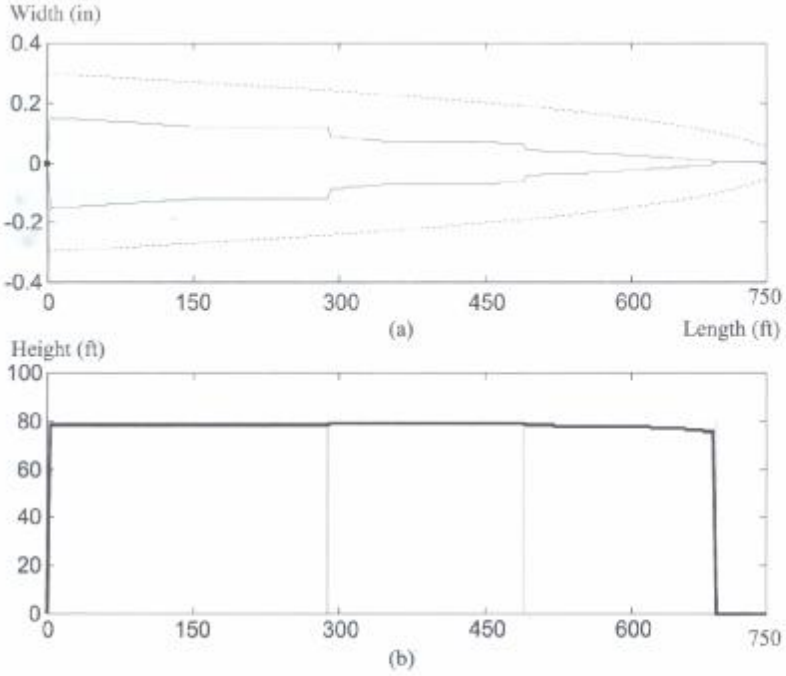

Fig. 5. Fracture width and height after closure for Case Study 1.

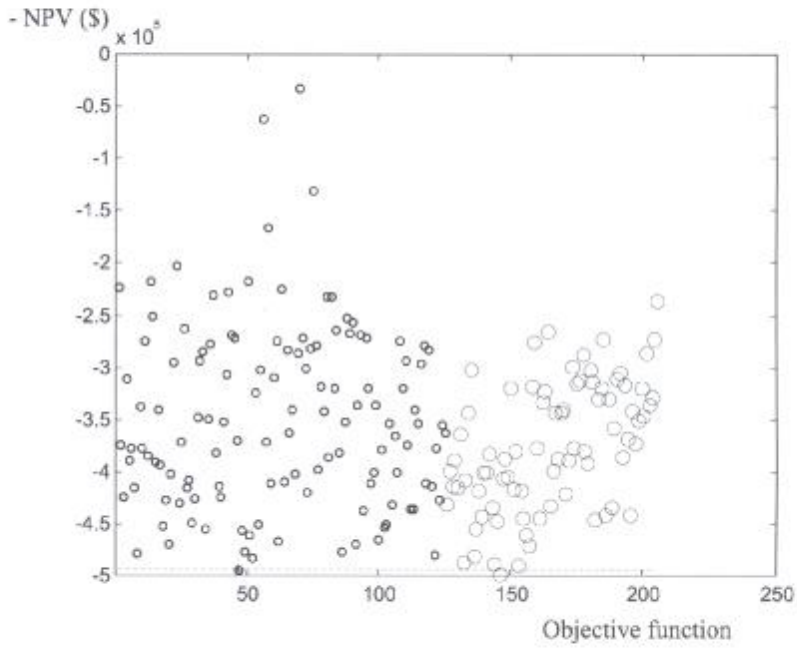

Fig. 6. Values of the objective function for Case Study 2.

input space was generated to construct the neural network (NN) and the DACE models. An additional sample of 50 points was generated to validate the NN model. The computational model was executed on all points to calculate, for each treatment, the objective function values. The minimum value obtained within the initial sample was -1.882×10^6 \$.

An NN with architecture $12 \times 1 \times 1$ was constructed and training and validation mean errors of 2.758×10^5 and 3.052×10^5, respectively, were obtained after only one training iteration. After the DACE model was estimated and validated, the NEGO algorithm added 80 points. Fig. 3 shows the plot of objective function values. The points represent the values corresponding to the initial sample while the circles correspond to points added by the NEGO algorithm. The dotted line indicates the objective function value for the best solution found within the initial sample. Among the points added by the NEGO algorithm, five (5) are better than the best solution found within the initial sample. Table 6 includes relevant information about these five points: number of iteration, input vector and objective function value. The best solution found corresponded to the 79th additional sampled point, and had an objective function value of -2×10^6 \$, which is 9.41% lower than the minimum value found in the initial sample. This point represents an increment of 1229% of the revenue when compared to the net present value of 1.79×10^5 \$, without executing the fracture treatment. Note that the best solution was obtained after 254 computationally expensive objective function evaluations.

For the overall best solution found, Fig. 4 shows the fracture width propagation during fluid injection.

Table 7
Best value of the objective function found by the NEGO algorithm (Case Study 2)

#Iter	V_1 (bbl)	V_2 (bbl)	V_3 (bbl)	V_4 (bbl)	V_5 (bbl)	ΔCp_{21} (lbm/gal)	ΔCp_{32} (lbm/gal)	ΔCp_{43} (lbm/gal)	ΔCp_{54} (lbm/gal)	Q_i (bpm)	n_p (–)	K_f (lbf s^{np}/ft^2)	$y \times 10^6$ (\$)
21	433.33	433.33	166.66	300.00	166.66	0.6667	2.00	2.00	2.00	43.33	0.650	0.0053	−4.991

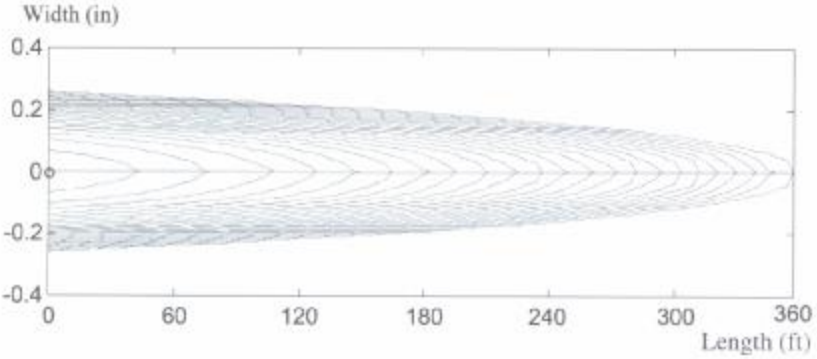

Fig. 7. Fracture width propagation during fluid injection for Case Study 2.

Each curve corresponds to a time step. Fig. 5(a) shows the width after fracture closure and, as a reference, the width after the fluid injection finishes (dotted line). Fig. 5(b) shows the height after fracture closure, which coincides with the trapped proppant height. The vertical lines represent proppant fronts. It should be noted that the proppant front locations correspond to width discontinuities due to changes in proppant concentrations between different stages.

5.2. Case Study 2

An initial sample of 125 was generated using a Latin hypercube experimental design to construct the

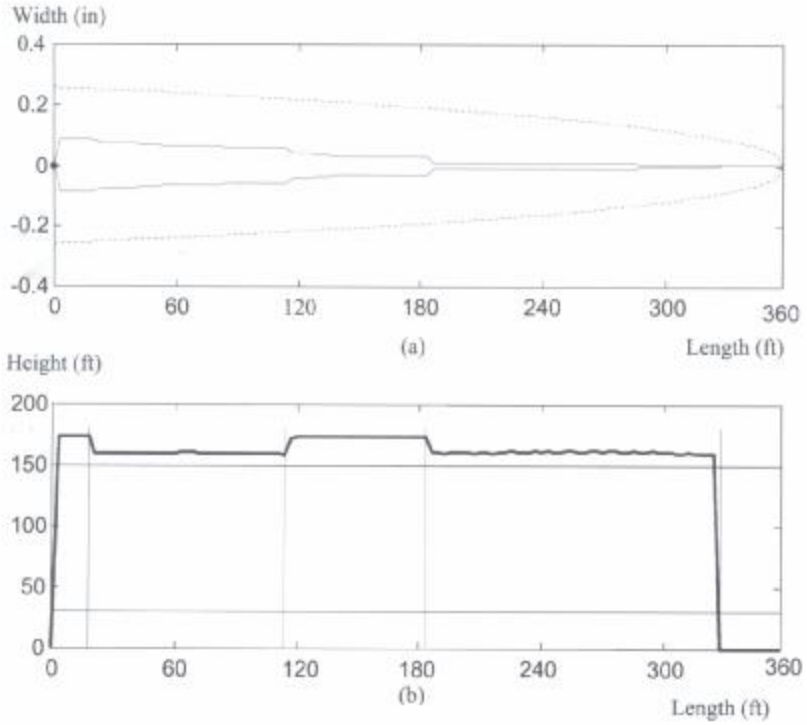

Fig. 8. Fracture width and height after closure for Case Study 2.

NN and the DACE models. An additional sample of 50 points was used to validate the NN model. The minimum value within the initial sample points was of -4.944×10^5.

An NN with architecture $12 \times 1 \times 1$ was constructed and training and validation mean errors of 8.5968×10^4 and 1.0002×10^5, respectively, were obtained after one training iteration. After the DACE model was estimated and validated, the NEGO algorithm added 50 points. Fig. 6 shows the plot of objective function values. The points represent the values corresponding to the initial sample while the circles correspond to points added by the NEGO algorithm. The dotted line indicates the objective function value for the best solution within the initial sample. Among the points added by the NEGO algorithm, one (1) is better than the best solution found within the initial sample. Table 7 includes the information about this point. This minimum objective function value, found in 21th iteration, had a value of -4.991×10^5 $, which is 9.91% lower than the best solution found within the initial sample. The best solution found represents an increment of 1800% of the revenue, when compared to the net present value (2.771×10^4 $) obtained without executing any fracture treatment. The best solution found was obtained after 146 evaluations of the objective function.

For the best overall solution found, Fig. 7 shows the fracture width propagation during fluid injection with each curve corresponding to a time step. Fig. 8(a) shows the width after fracture closure and the width after the fluid injection finishes (dotted line) and Fig. 8(b) shows the height after fracture closure (trapped proppant height). The vertical lines represent proppant fronts and the horizontal lines delimit the pay zone.

6. Conclusions

- A methodology for the optimal design of hydraulic fracture treatments has been proposed. The method includes the construction of a "fast surrogate" of an objective function, whose evaluation involves the execution of a time-consuming computational model, based on neural networks, DACE modeling and adaptive sampling. Using adaptive sampling, promising areas are searched considering the information provided by the surrogate model and the expected value of the errors.
- The optimization approach holds promise to be useful in the optimization of objective functions involving the execution of computationally expensive mathematical models and is expected to outperform competing methods, in terms of computationally expensive objective function evaluations, necessary to meet an stopping criteria. This is because it can identify promising areas without the need of moving step by step along a given trajectory. Additionally, by providing estimates of the errors at unsampled points, it is possible to establish a reasonable stopping criterion. Furthermore, it provides a fast surrogate model that could be used to visualize the relationship between the sought parameters and the objective function values and to identify the relative significance of each of the parameters.
- The methodology was tested on two case studies corresponding to formations differing in rock and fluid properties, and geometry parameters (12 parameters). The improvement revenues for the fracturing treatment solutions were 1229% and 1800% for the first and second case, using 305 and 225 objective function evaluations. The results suggest that the methodology can be used effectively and efficiently for the optimal design of hydraulic fracture treatments.

Nomenclature

A	Fracture vertical section area
a_i	Initial declination rate
B_o	Oil volumetric factor
C	Leak-off coefficient
COP	Cumulative oil production
Cp	Proppant concentration
$\overline{\text{Cp}}$	Normalized proppant concentration
D	Proppant diameter
DACE	Design and analysis of computer experiments
E	Young modulus
F	Objective function
$f_{\min}$	Current best function value
fom	Figure of merit
$\hat{f}$	DACE predictor
H	Fracture height
H_{eff}	Height of the propped fracture after closure
H_p	Height of the pay-zone

J	Productivity index after fracture
J_o	Productivity index before fracture
K_r	Reservoir permeability
K_f	Fluid consistency index
K_p	Proppant permeability
L	n-vector of ones
L0	Fracture length
NPV	Net present value
NPV_{rev}	Net present value of the revenue
NPV_{inc}	Net present value of the income
NPV_{cost}	Net present value of the costs
n_p	Fluid behavior index
P	Pressure
P_{wf}	Flowing bottomhole pressure
P_i	Reservoir initial pressure
$\bar{P}$	Average value of P_{wf} and P_i
P	vector $\boldsymbol{x}$ dimension
Q_i	Initial flow rate
Q_o	Oil production rate
Q_L	Fluid loses rate
Q_{of}	Initial oil production rate after fracture
R	Correlation matrix between the n sample points
$\boldsymbol{r}'$	Correlation vector between the new point and the points used to construct the model
r_e	Reservoir outer boundary radius
r_w	Well radius
S_p	Spurt-loss coefficient
$s^2(x)$	Mean square error of the predictor
T	Time horizon in years
V_i	Volume of the i-th injection stage
V_s	Proppant particles descent velocity
W	Fracture width
W_{eff}	Width of the propped fracture after closure
$\boldsymbol{x}$	Design vector
X	Set of constraints
y	DACE response value

Symbols

ΔCp_{ji}	Proppant concentration change between i-th and j-th stages
ε	Error in the DACE model
$\tau(x)$	Time for which the fracture opened at x
υ	Poisson ratio
η	Parameter related to the fluid viscosity
ρ_p	Proppant density
ρ_{f0}	Fluid density
μ	Mean of the population
μ_a	Apparent fluid viscosity
μ_o	Oil viscosity
σ	Standard deviation of the population
θ_h	Correlation parameter
Φ	Cumulative normal distribution function
ϕ	Density normal distribution function

Acknowledgements

The authors gratefully acknowledge the financial support provided to this project by the Consejo Nacional de Investigaciones Petroleras (CONIPET) and the Consejo Nacional de Investigaciones Científicas (CONICIT), Venezuela.

References

Balen, M.R., Meng, H.Z., Economides, M.J., 1988. Application of net present value (NPV) in the optimization of hydraulic fractures. SPE Paper 18541 presented at the SPE Eastern Regional Meeting in Charleston, USA, 181–191.

Daneshy, A., 1978. Numerical solution of sand transport in hydraulic fracturing. Journal of Petroleum Technology, 132–140. January.

Domselaar, H.R., Visser, W., 1974. Proppant concentration in a final shape of fractures generated by Viscous Gels. Society of Petroleum Engineers Journal, 531–536. December.

Geertsma, J., de Klerk, F., 1969. A rapid method of predicting width and extent of hydraulically induced fractures. Journal of Petroleum Technology 246, 1571–1581.

Hareland, G., Rampersad, P., Dharaphop, J., Sasnanand, S., 1993. Hydraulic fracturing design optimization. SPE Paper 26950 presented at the SPE Eastern Regional Conference and Exhibition help in Pittsburgh, PA, USA, 493–500.

Jones, D.R., Perttunen, C.D., Stuckman, B.E., 1993. Lipschitzian optimization without the Lipschitz constant. Journal of Optimization Theory and Applications 79 (1), 157–181.

Jones, D., Schonlau, M., Welch, W., 1998. Efficient global optimization of expensive black-box functions. Journal of Global Optimization 13, 455–492.

MATLAB, Ver. 5.3. The MathWorks.

Mohaghegh, S., Popa, A., Ameri, S., 1999. Intelligent systems can design optimum fracturing jobs. SPE Paper 57433 presented at the SPE Eastern Regional Meeting held in Charleston, West Virginia, USA, pp. 1–9.

Nolte, G.K., 1979. Determination of fracture parameters from fracturing pressure decline. SPE Paper 8341 presented al the SPE 54th Annual Fall Technical Conference and Exhibition held in Las Vegas, Nevada, USA, pp. 1–16.

Novotny, E.J., 1977. Propant Transport. SPE 6813 presented at the 52th Annual Fall Technical Conference and Exhibition of the

Society of Petroleum Engineers of AIME held in Denver, Colorado, USA, Oct. 9–12, pp. 1–12.

Poulsen, K.D., Soliman, M.Y., 1986. A Procedure for Optimal Hydraulic Fracturing Treatment Design. SPE Paper 15940 presented at SPE Eastern Regional Meeting held in Columbus, OH, USA, 221–230.

Queipo, N., Pintos, S., Contreras, N., Rincon, N., Colmenares, J., 2000. Surrogate Modeling—Based Optimization for the Integration of Static and Dynamic Data into a Reservoir Description. SPE Paper 63065 presented at the SPE Annual Technical Conference and Exhibition held in Dallas, Texas, USA, pp. 1–10.

Ralph, W., Veatch Jr., W. 1986. Economics of fracturing: some methods, examples and case studies. SPE Paper 15509 presented at SPE 61th Annual Technical Conference and Exhibition held in New Orleans, Atlanta, USA, pp. 1–16.

Raymond, L.R., Binder Jr., G.G. 1967. Productivity of wells in vertical fractured damaged formations. Journal of Petroleum Technology, 120–130 January.

Rueda, J.I., Rahim, Z., Holditch, S.A., 1994. Using a Mixed Integer Linear Programming Technique to Optimize a Fracture Treatment Design. SPE Paper 29184 presented at the SPE Eastern Regional Meeting held in Charleston, South Carolina, USA, pp. 233–244.

Sacks, J., Welch, W., Mitchell, T., Wynn, H., 1989. Design and analysis of computer experiments. Statistical Science 4, 409–435.